

## Simulation of Fault Detection in AC to AC Converter Fed Induction Motor

Nagarajan S.<sup>1</sup> and Rama Reddy S.<sup>2</sup>

<sup>1</sup>Research Scholar, <sup>2</sup>Professor,  
Electrical and Electronics Engineering Dept., Jerusalem College of Engineering,  
Center for Collaborative Research with Anna University, Chennai, India  
E-mail: [nagu\\_shola@yahoo.com](mailto:nagu_shola@yahoo.com), [srr\\_victory@yahoo.com](mailto:srr_victory@yahoo.com)

### Abstract

This paper presents simulation results of the harmonics analysis of motor current signatures under different fault condition of Voltage Source Inverter (VSI) fed induction motor drive. Simulation studies are performed for three different fault conditions i.e. open circuiting of one of gate of the six IGBTs, blowing off one IGBT and line to ground fault at one of the motor phase terminals. Under these fault conditions, time domain and frequency domain analyses are performed and the simulation results are presented.

**Keywords:** Induction Motor, FFT Spectrum, THD, Faults at IGBT.

### Introduction

Induction Motor for many years has been regarded as workhouse in industrial applications. In the last few decades induction motor has evolved from being a constant speed motor to variable speed, variable torque machine. When the application requires large power and torque specifications, the usage of induction motor comes into demand. This results in application of an efficient machine which is stable during various fault conditions.

Hence machine fault detection becomes an important factor of concern. In past decades a number of different incipient fault detection methods and schemes have been presented. A Review of Induction Motors Signature Analysis as a Medium for Faults Detection (Benbouzid M.E.H) deals with a concise manner the fundamental theory, main results, and practical applications of motor signature analysis for the detection and the localization of abnormal electrical and mechanical conditions that indicate, or may lead to, a failure of induction motors [1]. Current Harmonics Analysis of Inverter-Fed Induction Motor Drive System under Fault Conditions (*Biswas B.*)

deals with harmonic analysis of motor current signatures under different fault conditions of medium and high power Variable Frequency Drive (VFD) systems. Computer simulation of a VSI fed induction motor based on constant voltage/frequency (V/f) operation is implemented using Powersim (PSIM) simulation software [2].

Simple Stator Fault Detector for AC Motors (Bin Huo) proposes a simple stator fault detector for ac motors, based on the TMC320C243 DSP controller is presented. The detector provides compensation of the constructional and supply voltage imbalances, and senses the ripple of the compensated instantaneous power [3]. Load-Commutated SCR Current-Source-Inverter-Fed Induction Motor Drive With Sinusoidal Motor Voltage and Current (Debmalya Banerjee) proposes a CSI-fed induction motor drive scheme where GTOs are replaced by thyristors in the CSI without any external circuit to assist the turning off of the thyristors [4]. Voltage Stresses on Stator Windings of Induction Motors Driven by IGBT PWM Inverters (Don-Ha Hwang) describes the distribution characteristics of switching the surge voltage in the stator windings of an induction motor driven by IGBT PWM inverter [5]. Online Diagnosis of Induction Motors Using MCSA (Jee-Hoon Jung) presents an online induction motor diagnosis system using motor current signature analysis (MCSA) with advanced signal-and-data-processing algorithms is proposed. MCSA is a method for motor diagnosis with stator-current signals [6],[10]. Motor Current Signature Analysis and Fuzzy Logic Applied to the Diagnosis of Short-Circuit Faults in Induction Motors (Luís Alberto Pereira) presents the development and the practical implementation of a system for detection and diagnosis of interturn short-circuits in the stator windings of induction motors. [7],[9]. Modeling And Simulation of the Three-Phase Induction Motor Using Simulink (Shi K. L.) describes a generalized model of the three-phase induction motor and its computer simulation using MATLAB/SIMULINK. Constructional details of various sub-models for the induction motor are given and their implementation in SIMULINK is outlined [8]. The above literature does not deal with simulation of faults in the 3-phase converter/inverter fed Induction Motor drive. This work deals with the faults in rectifier and inverter circuits of induction motor drive solid state system.

### **VSI-FED Induction Motor Drive**

An inverter, in which the input voltage is maintained constant, is called as Voltage fed inverter. The variable frequency drives operate by converting a three-phase voltage source to DC using rectifier. After the power flows through the rectifiers it is stored on a dc bus. The dc bus contains capacitors to accept power from the rectifier, stores it, and later deliver that power through the inverter section. The inverter contains transistors that deliver power to the motor. The “Insulated Gate Bipolar Transistor” (IGBT) is a common choice in modern VFDs. The IGBT can switch on and off several thousand times per second and precisely control the power delivered to the motor. The IGBT uses “pulse width modulation” (PWM) technique to supply a sine wave current at the desired frequency to the motor. A variable output voltage can be obtained by varying the input DC voltage and maintaining the gain of the inverter

constant. On the other hand if the DC input voltage is not constant and is not controllable, a variable voltage can be obtained by varying the gain of the inverter by pulse-width modulation (PWM) control within the inverter.

In industrial complexes, many induction motors, may often be running at no load or partial load. Hence, Proper fault analysis is needed to obtain an efficient machine. This work deals with harmonic analysis of motor current signatures for the following types of faults: open circuiting of one of the six IGBTs gate, blowing off one IGBT, line to ground fault at one of the motor phase terminals. The faults are being introduced in inverter and rectifier modules of the VSI fed induction motor drive.

## Simulation Results

The circuit for the detection of faults for three phase induction motor is simulated by using MATLAB.

### *Without Fault*

The Simulink circuit of VSI fed induction motor drive without fault is shown in Fig.1. The 415V AC voltage is applied to the drive system.

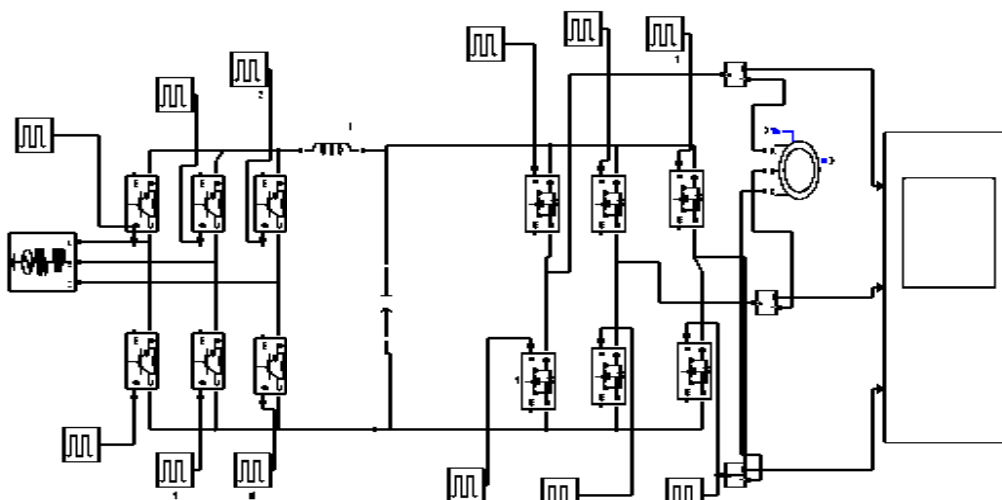


**Figure 1:** Simulink model of VSI-fed induction motor drive without fault.

The waveforms of line currents under the healthy conditions are shown in Fig.2. It is observed that the current is 38A under healthy condition.

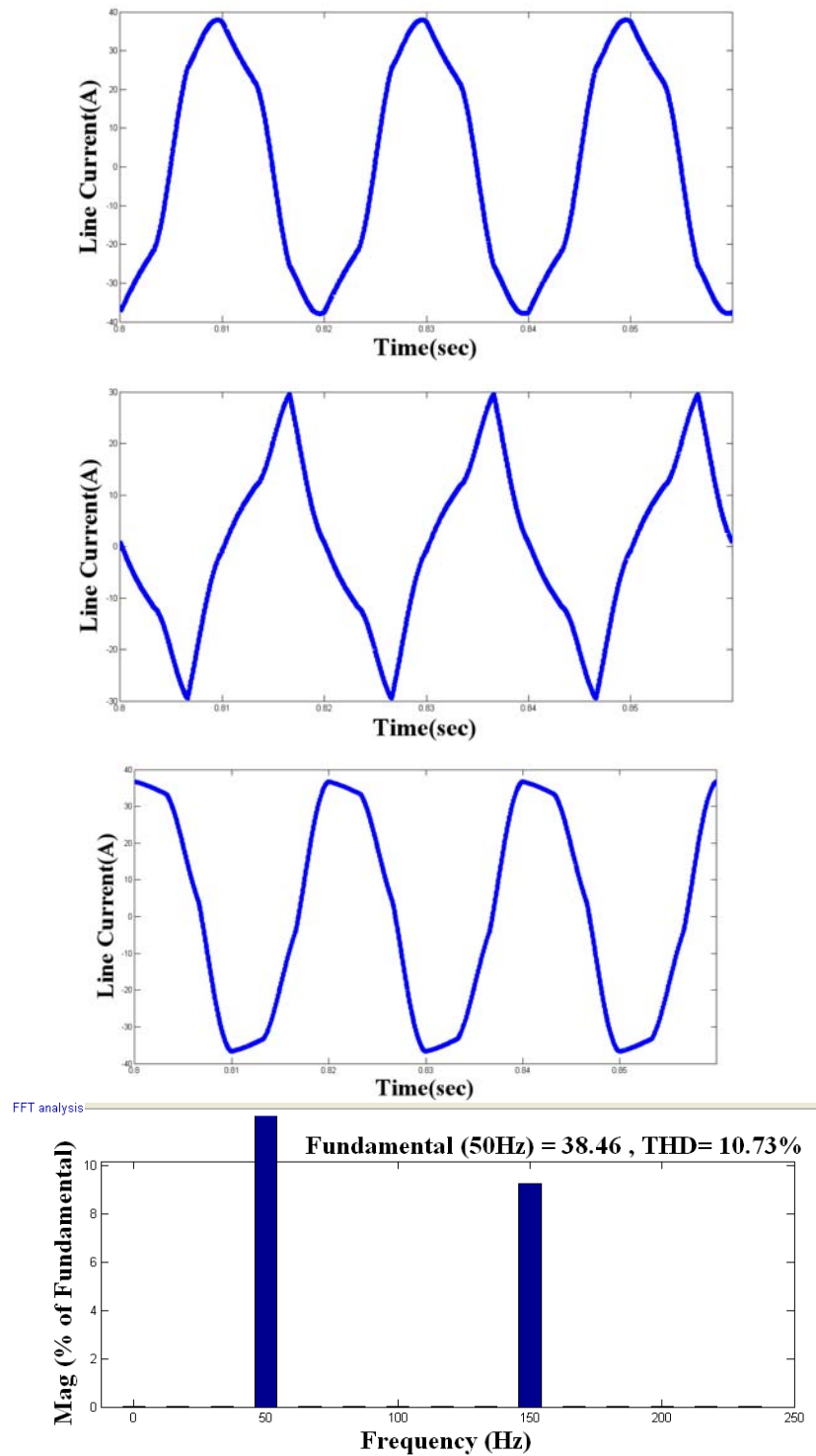


**Figure 2:** Line Current Waveforms & Line Spectrum under healthy condition Line current waveform of (a) Phase A (b) Phase B (c) Phase C (d)Line spectrum under healthy condition

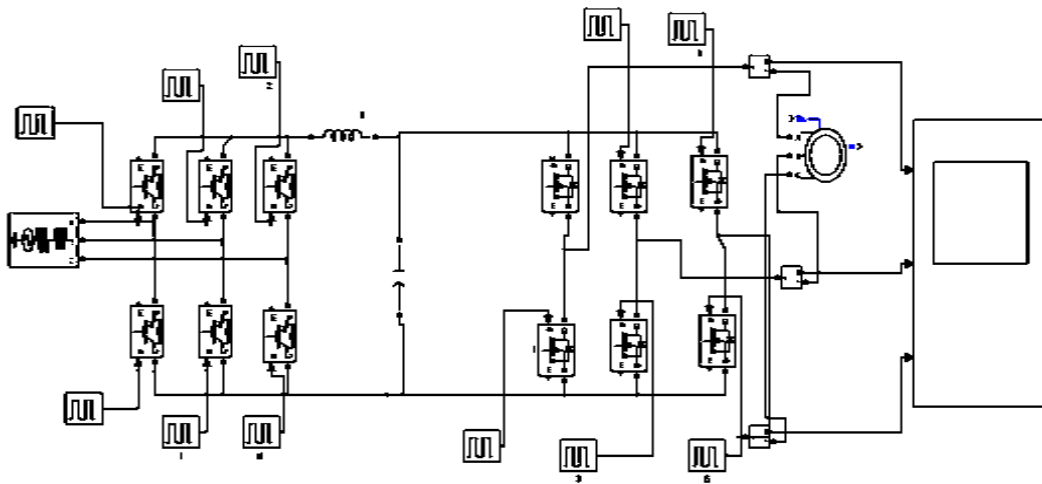
The line current spectrum under the healthy condition is shown in Fig. 2. The THD value is 10.73%.

### ***Faults in Inverter***

In this section various faults are introduced in the inverter of the VSI-fed drive.

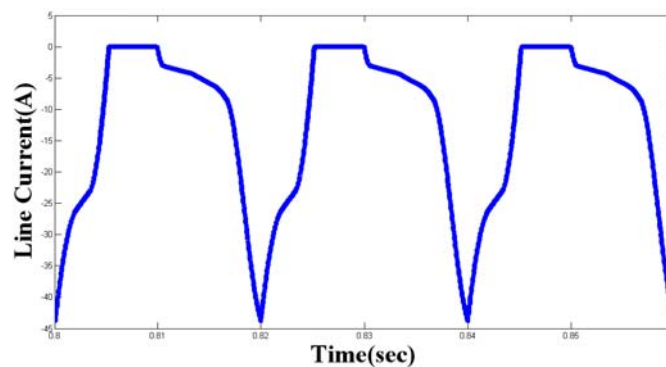
#### ***Open circuiting IGBTs gate terminal***

In the inverter the pulse input to the upper IGBT in first leg is absent. The Simulink circuit for this fault is shown in Fig. 3.



**Figure 3:** Simulink model with Ph A IGBT open circuited in inverter.

The waveforms of line currents of the three phases under the fault conditions are shown in Fig 4. It is observed that current direction gets reversed in Phase A. The current is measured as 43A. The Phase currents  $I_b$  &  $I_c$  are distorted under open circuit fault condition.



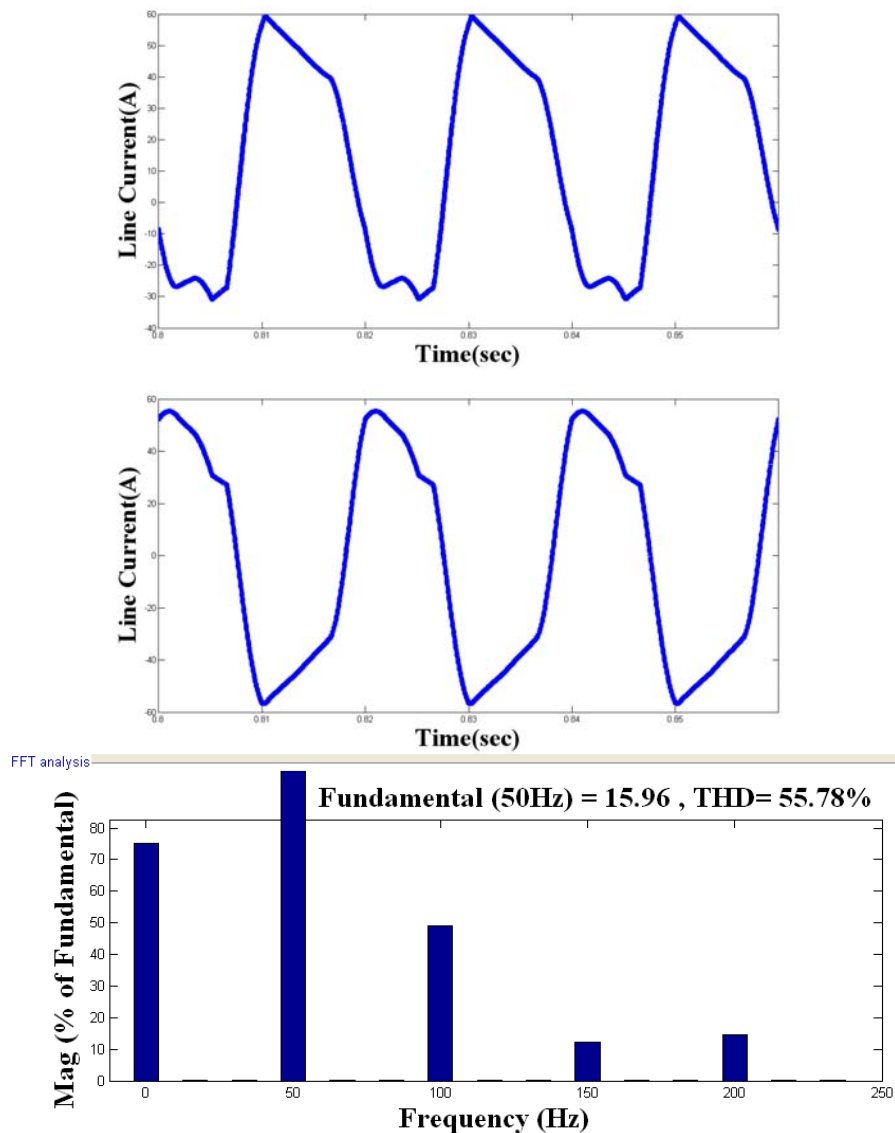
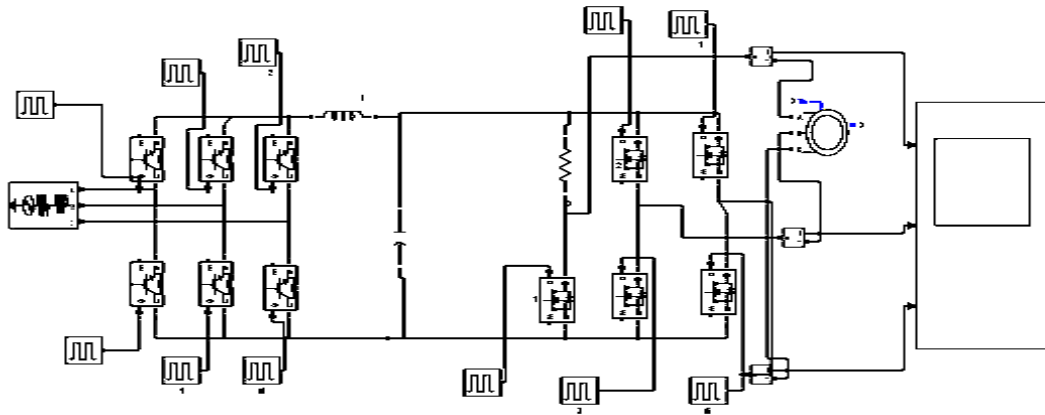


**Figure 4:** Line Current Waveforms & Line Spectrum with Ph A IGBT open circuited in inverter Line current waveforms of (a) Phase A (b) Phase B (c) Phase C (d)Line spectrum with Ph A IGBT open circuited in inverter

The line spectrum with Ph A IGBT open circuited in the inverter is shown in Fig. 4. The THD value is 55.78%. The THD increases by 5 times with respect to healthy condition.

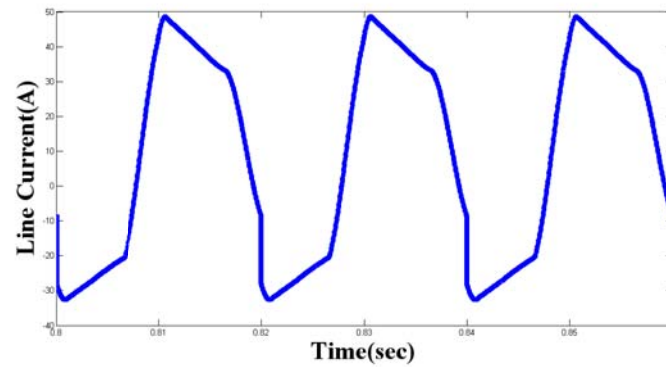
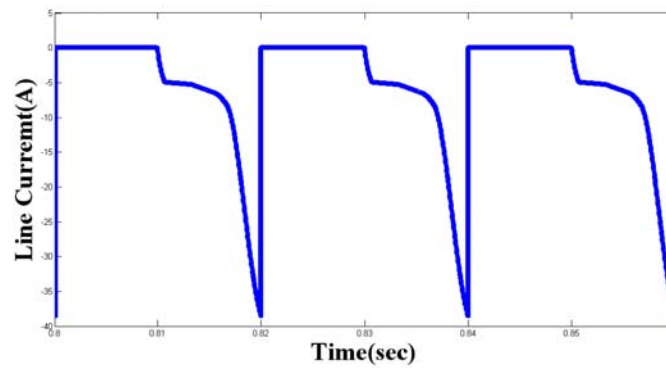
#### ***Blowing off one IGBT in the inverter module***

To simulate this condition, the upper IGBT in the phase A has been replaced by a high resistance of 1Mega Ohms. The Simulink circuit is shown in Fig.5.



**Figure 5:** Simulink model with Ph A IGBT blown off in inverter.

The waveforms of line Current of the three phases under fault condition are shown in Figs.6a, 6b &6c respectively. From the simulation results it is observed that Ph A current direction gets reversed and the current is 38A. The Phase currents  $I_a$  &  $I_c$  are distorted under fault condition.



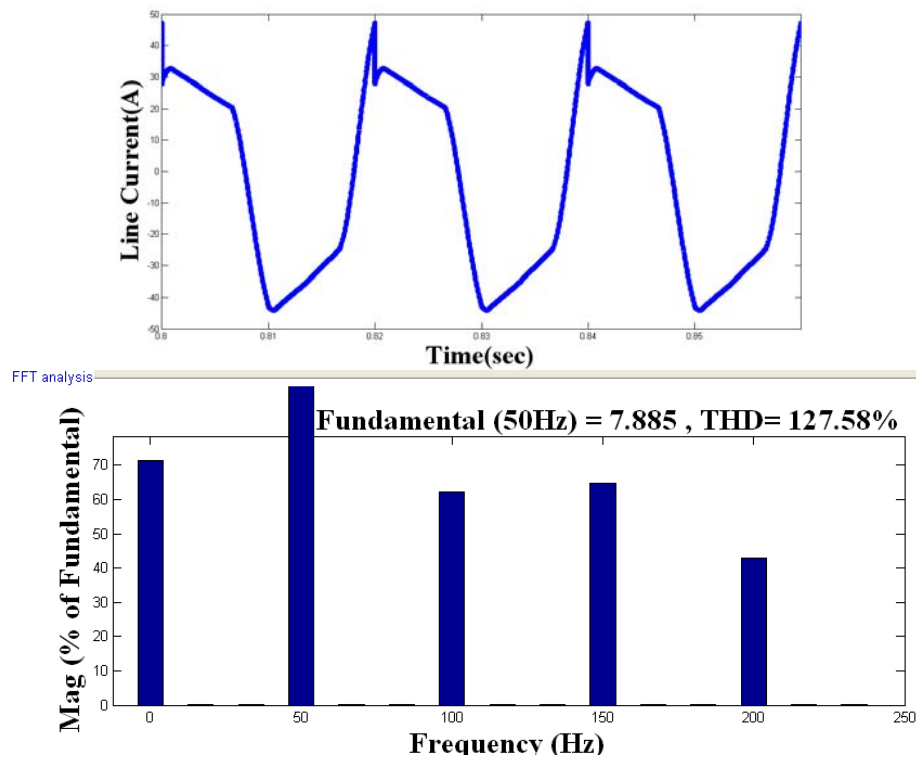


**Figure 6:** Line Current Waveforms & Line Spectrum with Ph A IGBT blown off in inverter Line current waveform of (a) Phase A (b) Phase B (c) Phase C (d)Line spectrum with Ph A IGBT blown off in inverter

The line spectrum with Ph A IGBT open circuited in inverter is shown in Fig. 6d. The THD value is 127.58%. The THD increases by 12 times with respect to healthy condition.

### ***Faults in Rectifier***

In this section various faults are introduced in the rectifier of the VSI-fed drive system.

### ***Source Current Waveforms without Fault***

The source current Vs time waveforms under healthy condition are shown in Fig. 7. It is observed that the current is 13A under healthy condition.



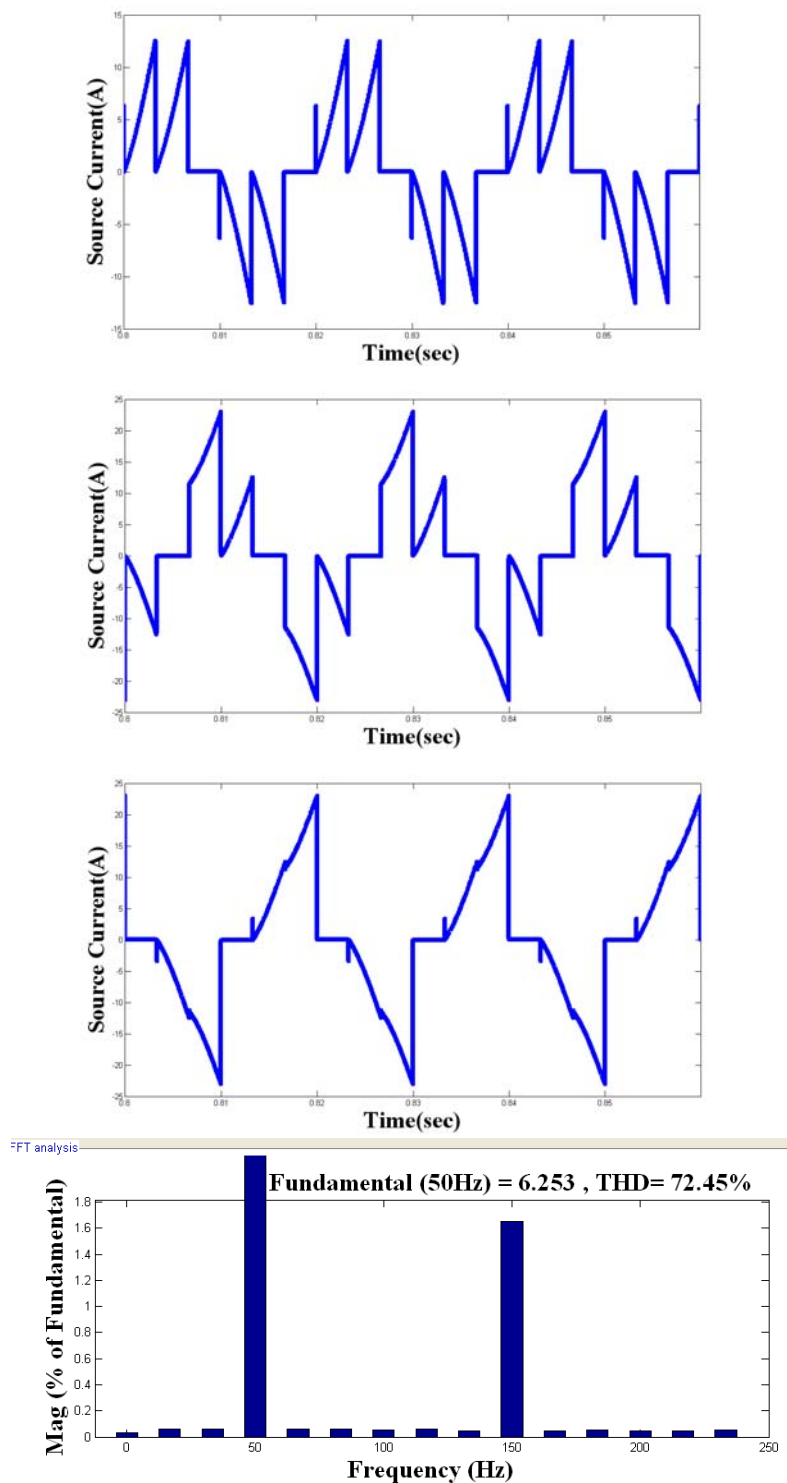
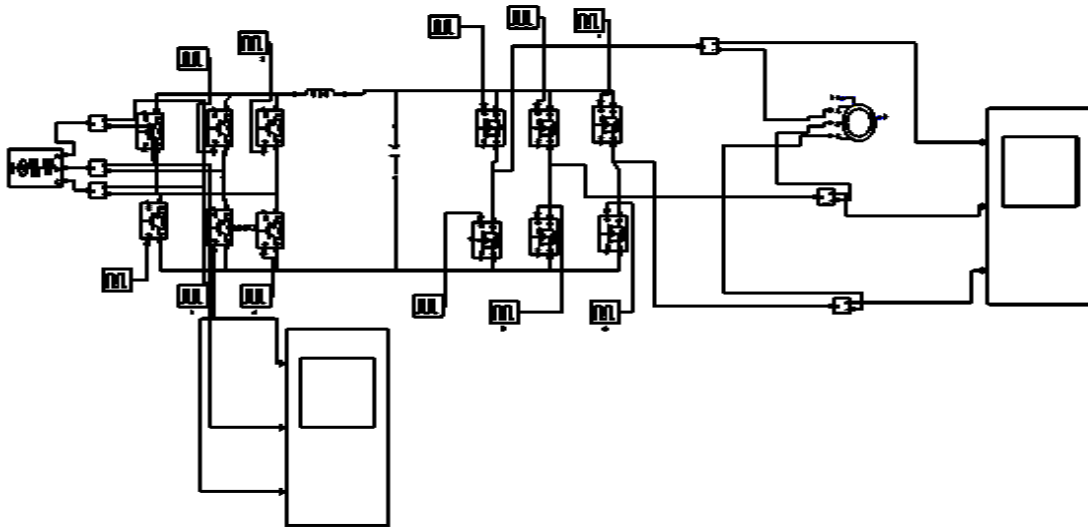


**Figure 7:** Source Current Waveforms & Line Spectrum in healthy condition Source current waveforms of (a) Phase A (b) Phase B (c) Phase C (d) Line spectrum in healthy condition.

The spectrum for source current under healthy condition of rectifier is shown in Fig. 7. The THD value is 72.45%.

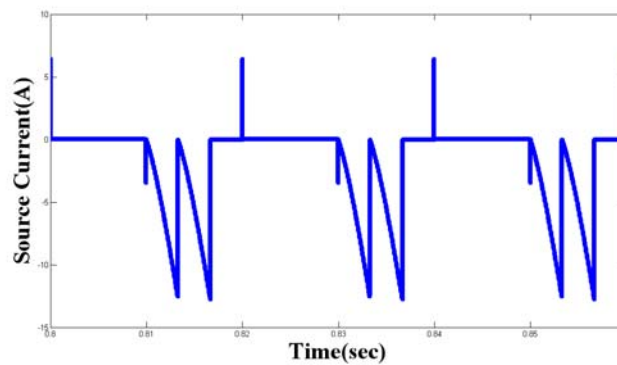
***Open circuiting of one of the six IGBTs gate terminal***

In rectifier the pulse input of upper IGBT in phase A is absent. The Simulink circuit is shown in Fig. 8.



**Figure 8:** Simulink model with Ph A IGBT open circuited in rectifier.

The source current waveforms of three phases A, B & C under fault condition are shown in Fig. 9. From the simulation results it is observed that the current direction gets reversed due to fault. The current is 13A.



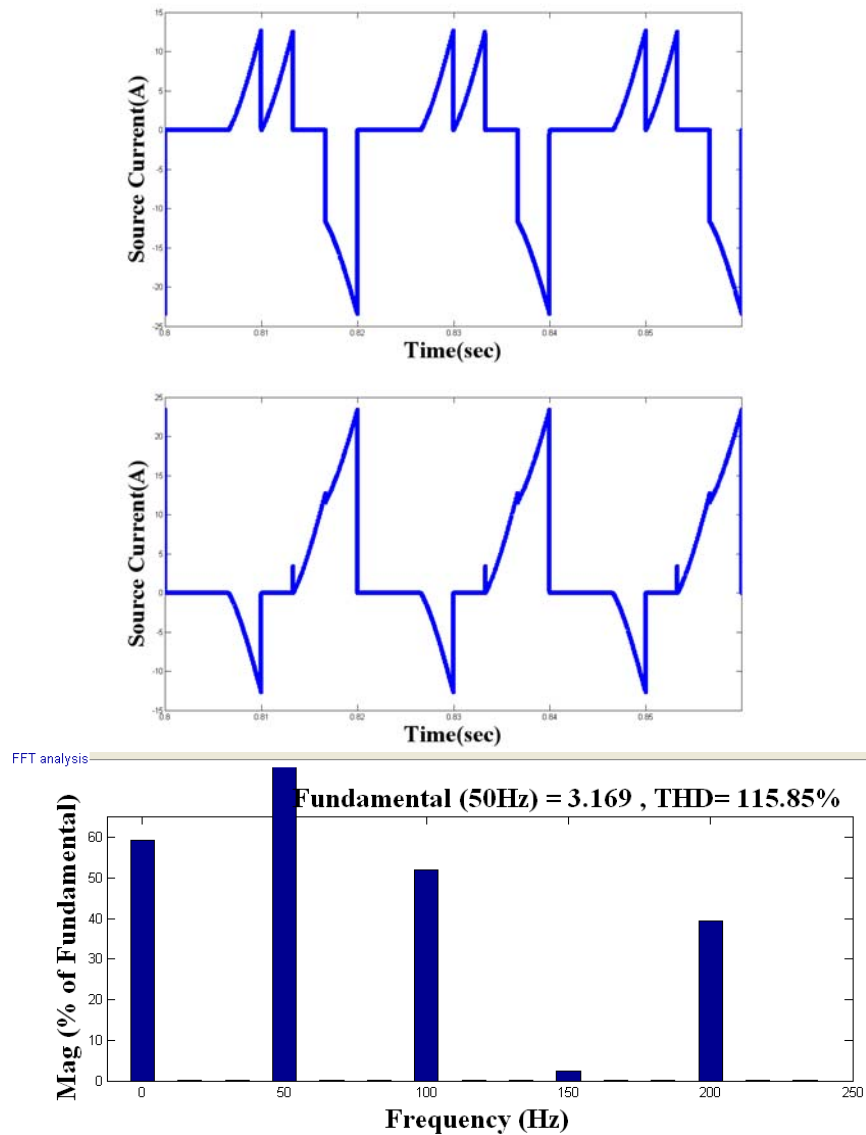
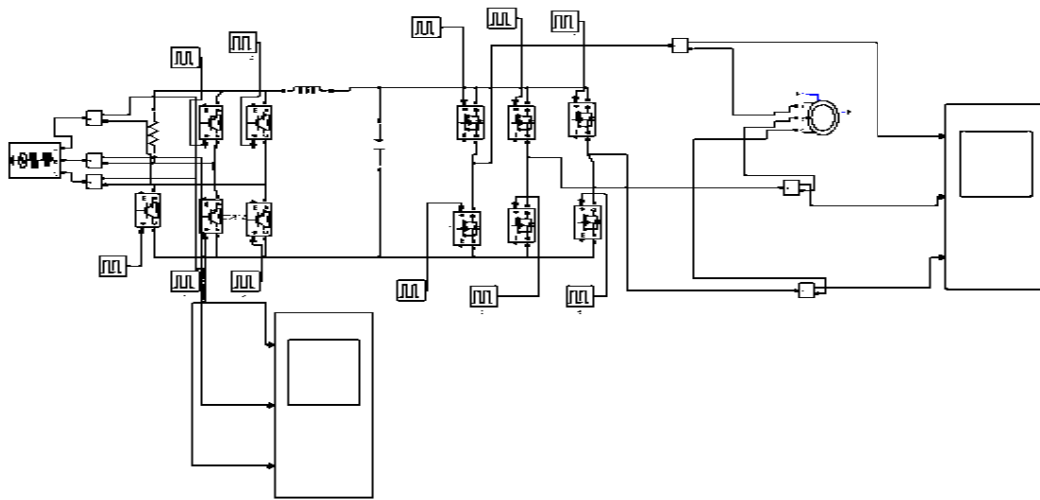


**Figure 9:** Source Current Waveforms & Line Spectrum with Ph A IGBT open circuited in rectifier Source current waveform of (a) Phase A (b) Phase B (c) Phase C(d)Line spectrum with Ph A IGBT open circuited in rectifier

The Line spectrum with Ph A IGBT open circuited in rectifier is shown in Figure 9. The THD value is 115.85%. The THD increases by 1.6 times with respect to healthy condition.

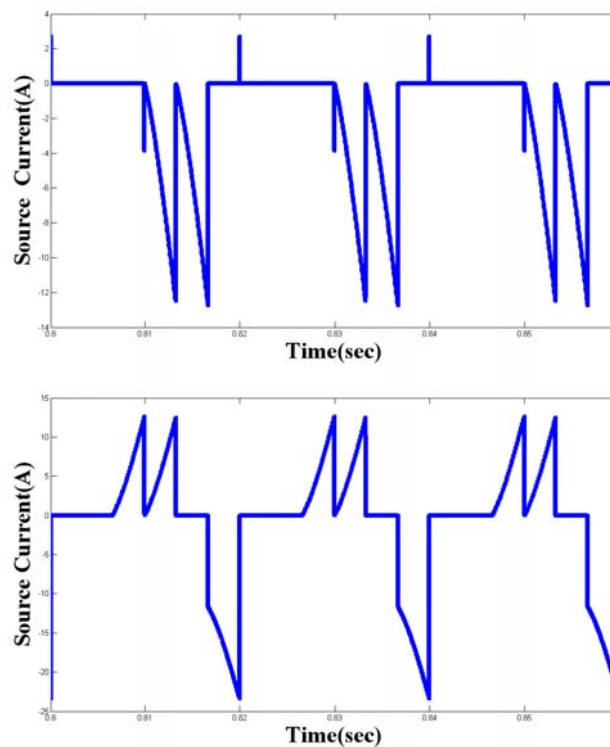
***Blowing off one IGBT in the rectifier module***

To simulate this condition, the upper IGBT in the phase A has been replaced by a high resistance of the order of Mega Ohms. The Simulink circuit is shown in Fig.10.



**Figure 10:** Simulink model with Ph A IGBT blown off in rectifier.

The waveforms of source current of the three phases A, B & C under the fault condition are shown in Fig 11. From the simulation results it is observed that the current direction gets reversed due to fault. The current is 13A. The current waveforms  $I_b$  &  $I_c$  are distorted under fault condition.



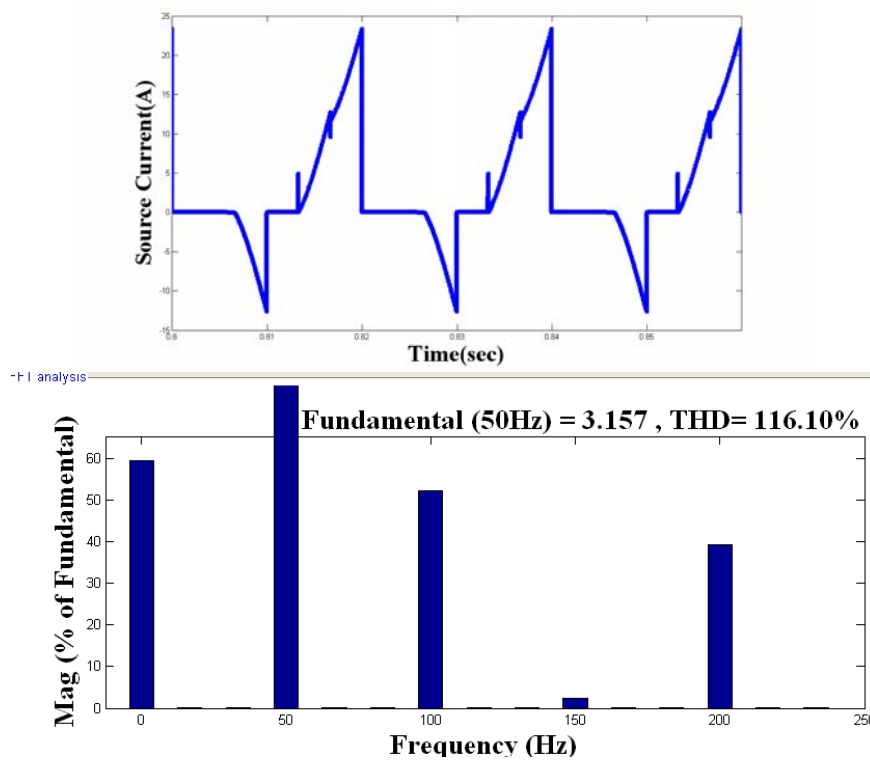
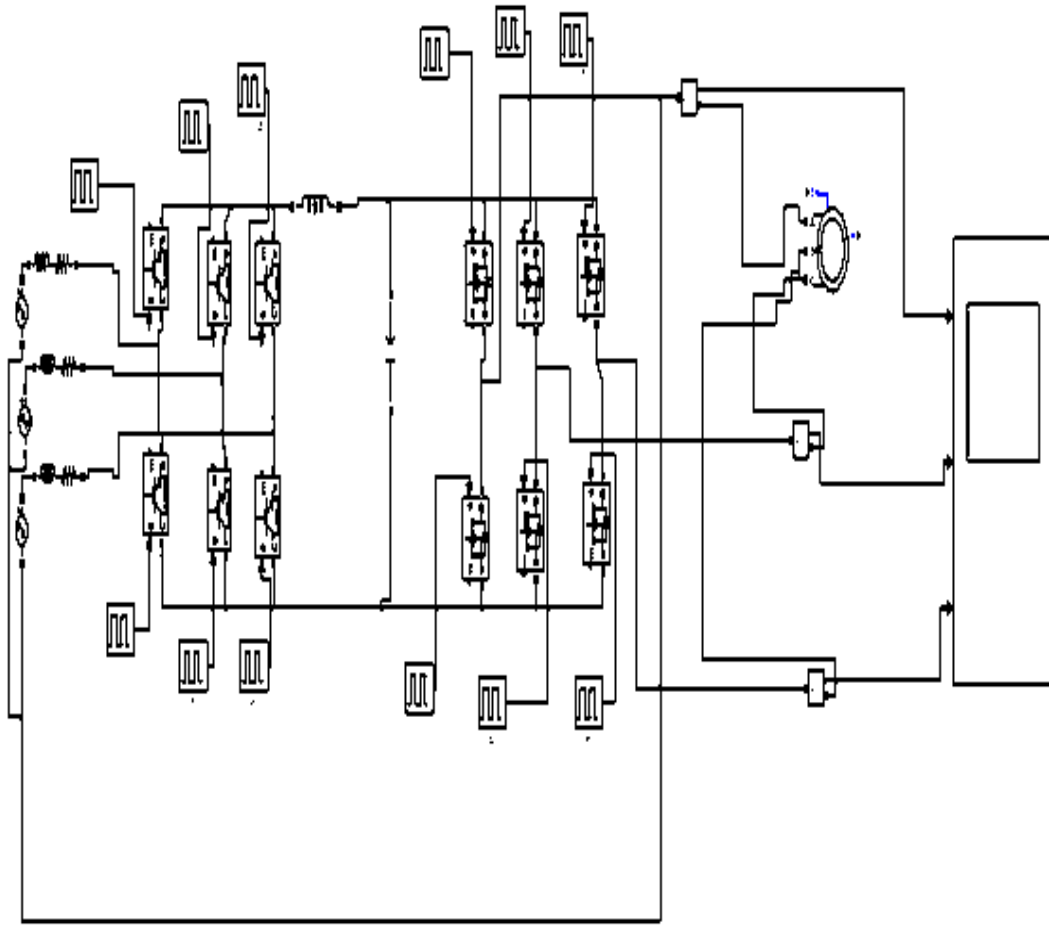


**Figure 11:** Source Current Waveforms & Line Spectrum with Ph A IGBT blown off in rectifier Source current waveform of (a) Phase A (b) Phase B (c) Phase C (d)Line spectrum with Ph A IGBT blown off in inverter

The Line spectrum with Ph A IGBT blown off in rectifier is shown in Figure 11. The THD value is 116.10%. The THD increases by 1.6 times with respect to healthy condition.

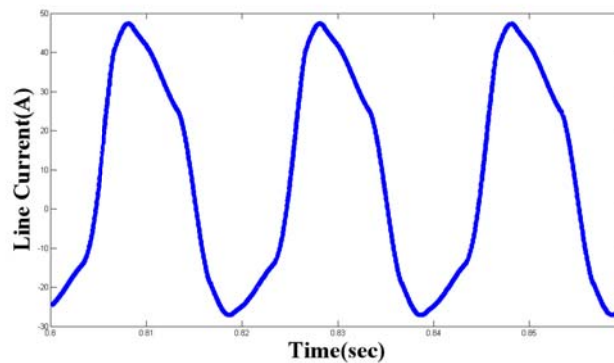
### ***Line to Ground Fault***

In this case the lower terminals of three sources are connected together to form a neutral. Neutral is connected to the line of motor load. The Simulink circuit is shown in Fig. 12.



**Figure 12:** Simulink model with Line to Ground Fault.

The waveforms of line current of the three phases A, B & C under the fault conditions are shown in Fig.13. From the simulation it is observed that line current waveforms get distorted due to line to ground fault. The current magnitude increases due to this fault. The magnitude of current is 48A.



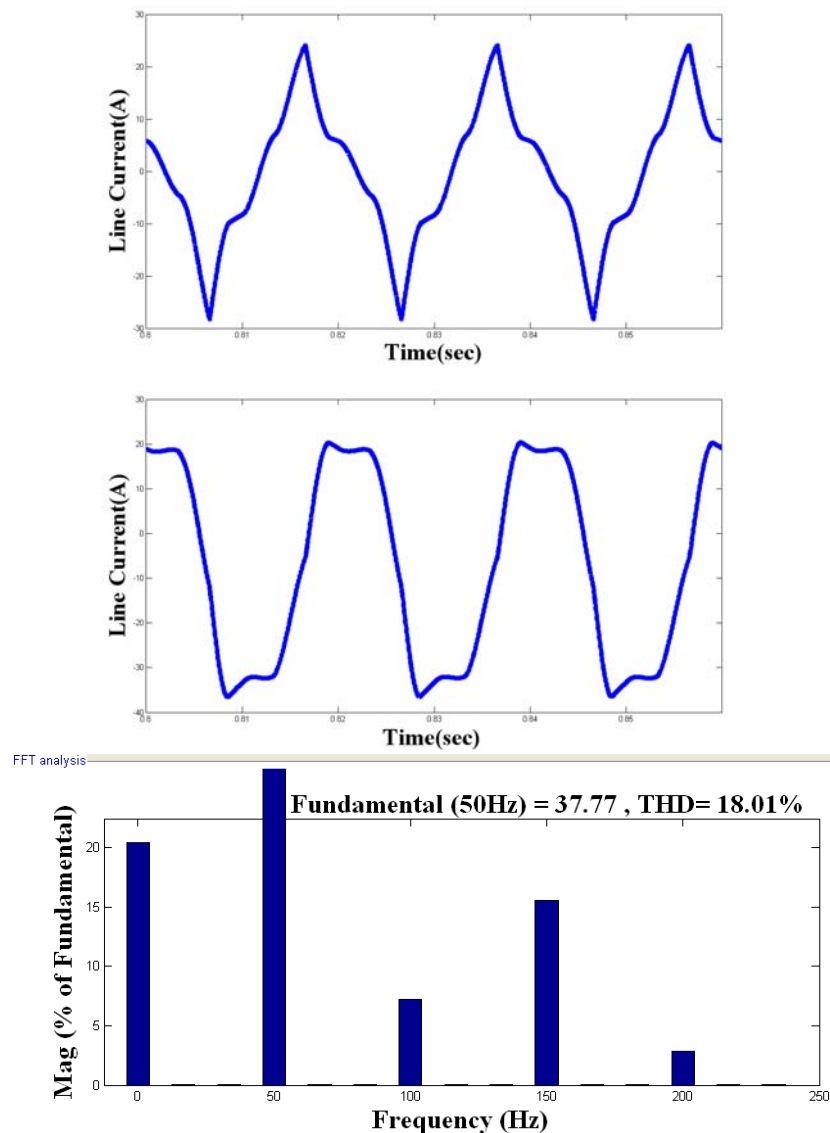


**Figure 13:** Line Current Waveforms & Line Spectrum with Line to Ground fault Source current waveform of (a) Phase A (b) Phase B (c) Phase C(d)Line spectrum with Line to Ground fault

The line spectrum with line to ground fault is shown in Fig. 13. The THD value is 18.01%. The THD increases by 1.6 times with respect to healthy condition.

The Summary of FFT analysis of VSI-fed Induction motor drive is given in Table 1. It can be observed that in inverter module, THD due to Ph A IGBT gate open circuit condition increases by 5 times and due to Ph A IGBT blown off increases by 12 times. In rectifier module, THD due to Ph A IGBT gate open circuited and due to Ph A IGBT blown off increases by 1.6 times. For Line to Ground fault, THD increases by 1.6 times. When faults are introduced in inverter module, the magnitude of current

increases for Ph A IGBT gate open circuited condition and current magnitude remains same for Ph A IGBT blown off condition. When faults are introduced in rectifier module, the current remains same. Due to faults the current direction gets reversed in inverter and rectifier modules. Due to line to ground fault, the currents increase by 1.3 times that of healthy condition.

**Table 1:** Summary of FFT Analysis.

CONDITION	THD (%)	CURRENT(Ampere)
<i>INVERTER MODULE</i>		
1. Without Fault	10.73	38
2. Phase A IGBT Open-Circuited	55.78	43
3. Phase A IGBT Blown off	127.58	38
<i>RECTIFIER MODULE</i>		
4. Without Fault	72.45	13
5. Phase A IGBT Open- Circuited	115.85	13
6. Phase A IGBT Blown off	116.10	13
<i>LINE to GROUND Fault</i>		
	18.01	48

## Hardware Description

The hardware design involves the following sections

- Power Supply Circuit.
- Driver Circuit
- Controller Circuit
- Power Circuit

An AC voltage of 230V is fed to the power supply circuit comprising ICs 7805 and 7812 to obtain required DC output voltages. The 5V DC output voltage obtained from regulator IC 7805 is given to the controller circuit and 12V DC output voltage obtained from regulator IC 7812 is given to the driver circuit. The control circuit comprising of Microcontroller AT89C51 and IR2110 which decides the sequence of pulses to be given to the switches in the power circuit. The driver circuit amplifies the pulses to the required level. The power circuit is an arrangement of six MOSFET switches (IRF530) with an input AC supply (230V/24V). The gate terminals of the switches are triggered according to the output frequency requirements. The block diagram of the hardware design is as shown in the Fig.14



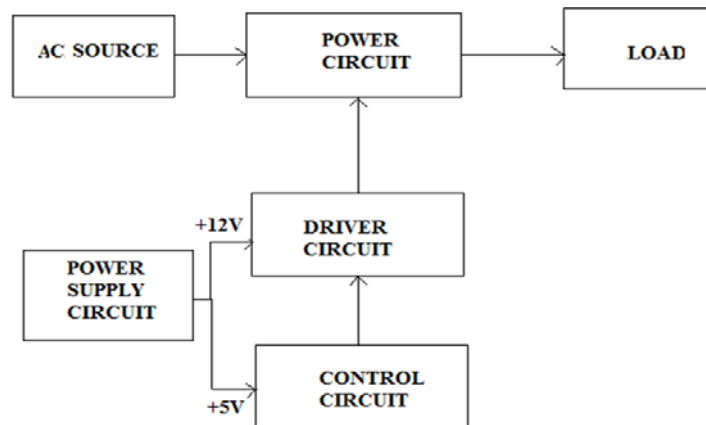


**Figure 14:** Block Diagram.

### Power Supply Circuit

The circuit consists of the following components

- Transformer
- Bridge rectifier
- Filter
- IC Regulator

The power supply section of hardware unit is shown in Fig. 15.

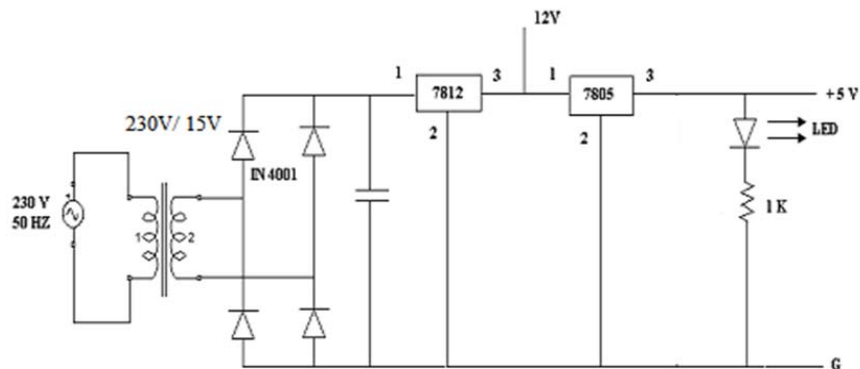


**Figure 15:** Power Supply Unit.

### Driver Circuit

The driver circuit is used for the purpose of isolation of negative current to the micro-controller, amplification of voltage and to create constant voltage source. The driver circuit diagram is shown in Fig. 16. The square pulse should have a constant voltage of 5V. This voltage is connected to isolator for isolation purposes. Isolation refers to separation of the power circuit from micro-controller. The output voltage from

microcontroller is given to IR2110 driver IC, the output voltage will have an increased magnitude that will be sufficient for driving the MOSFET IRF530.

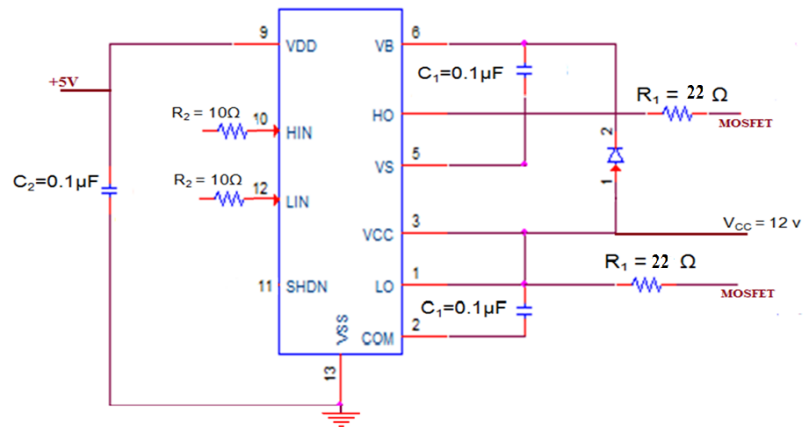


**Figure 16:** Driver Circuit.

### Controller Circuit

The main part of the hardware circuit is the Micro controller AT89C51. A suitable program is written in the controller to generate a train of pulses. In the control circuit, a Microcontroller is used. The driving pulse required for the MOSFETs IRF530 is obtained from this controller. AT89C51 IC is used. The circuit diagram of microcontroller is shown in Fig. 17.

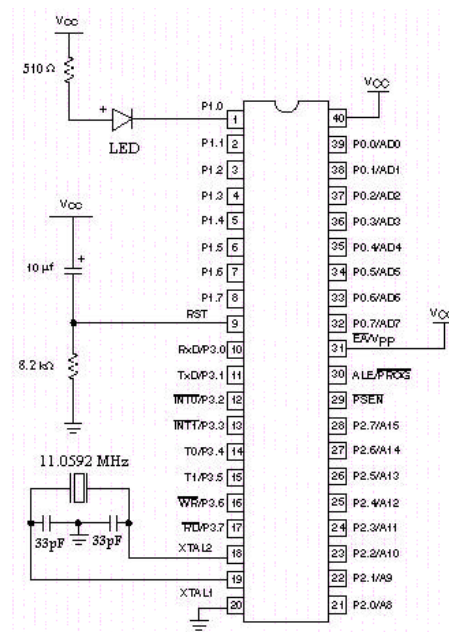


**Figure 17:** Controller Circuit.

### Power Circuit

The power circuit is three phase inverter and the supply to this circuit is given from a transformer 230/24V where 24V is applied to the circuit. The MOSFETs (IRF530) are connected in the required fashion. The gate pulses are given from the driver circuit. Load resistance of 1kohm is provided. The power circuit is shown in Fig. 18. The inverter switching sequence is shown below in Table 2.

**Table 2:** Switching Sequence of Driving Signals.

Sequence	S1	S2	S3	S4	S5	S6
I	1	0	0	0	1	1
II	1	1	0	0	0	1
III	1	1	1	0	0	0
IV	0	1	1	1	0	0
V	0	0	1	1	1	0
VI	0	0	0	1	1	1

**Switch State: 0-Open,1-Closed**

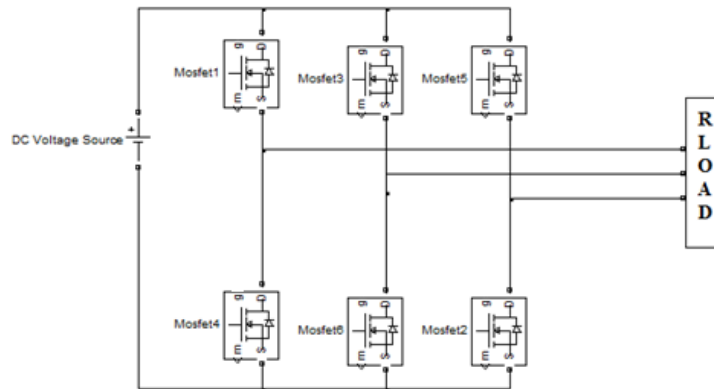


**Figure 18:** Power Circuit.

### Complete Hardware Circuit

The complete hardware circuit is shown in the Fig. 19.

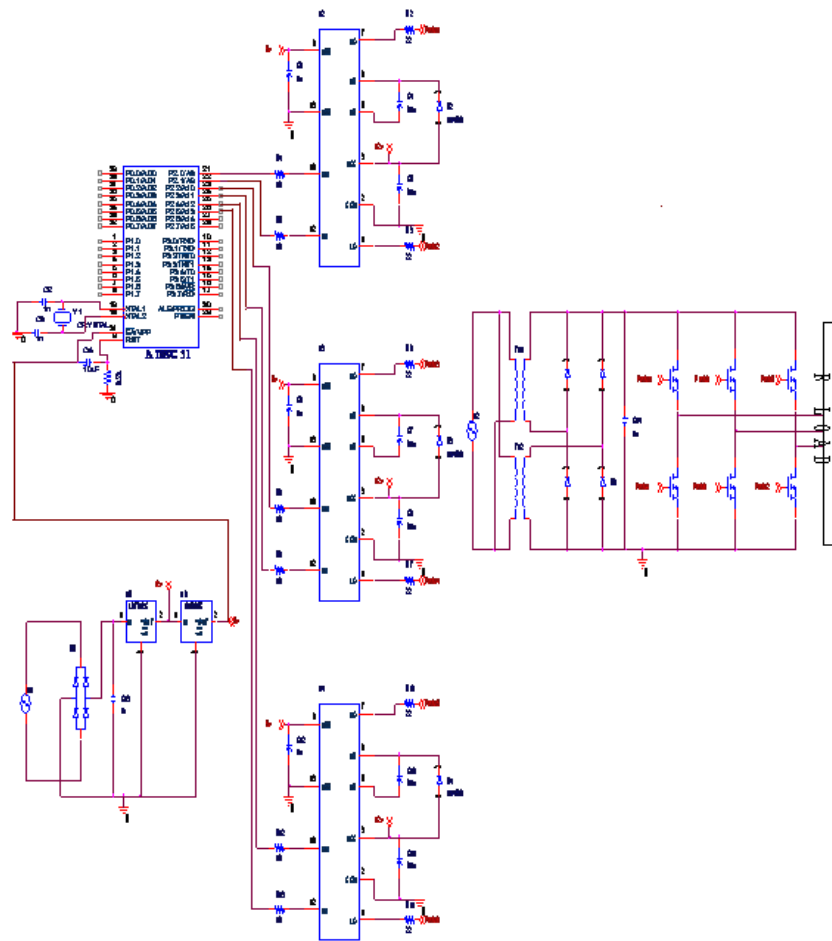
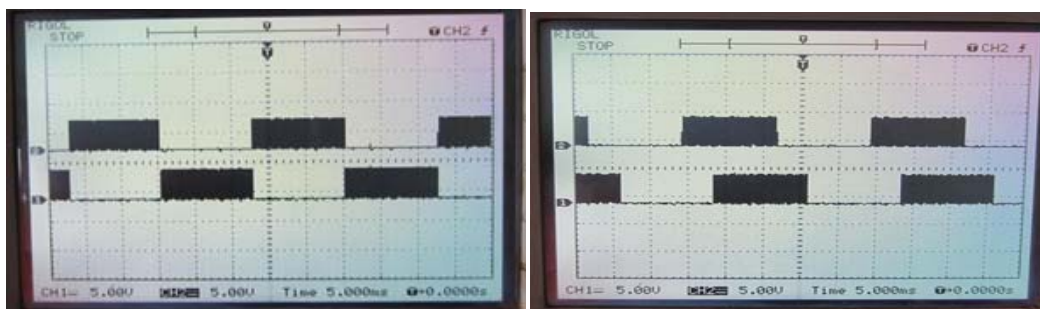


**Figure 19:** Complete Hardware Circuit.

**Testing**

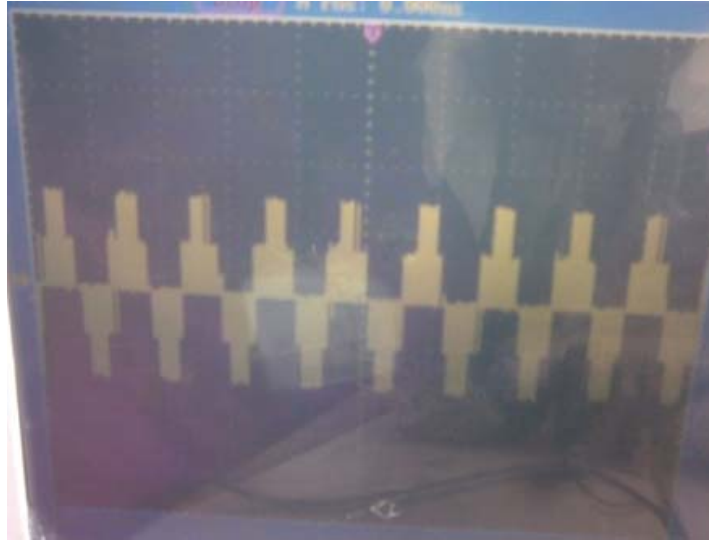
The output waveforms from Controller Circuit, Power Circuit and the Complete Hardware Setup is shown in Fig. 20, 21 and 22.



X axis, 1cm=5ms

Y axis, 1cm=5V

**Figure 20:** Output from Controller.



X axis, 1 cm=5ms, Y axis, 1cm=20V

**Figure 21:** Output from Power circuit.

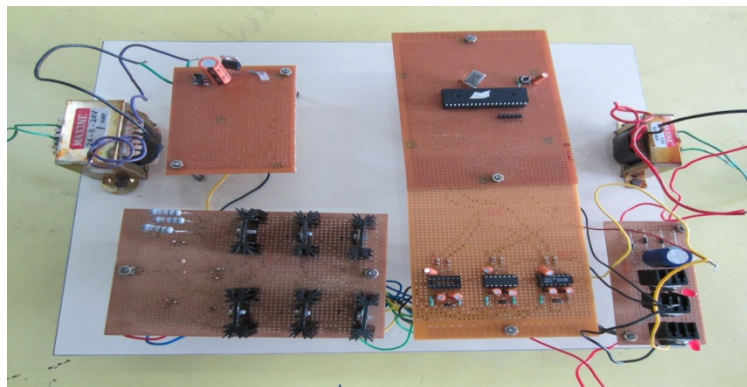


**Figure 22:** Complete Hardware Setup.

## Conclusion

In this paper, the THDs of VSI-fed drives are evaluated under various fault conditions of rectifier and inverter circuits. Output waveforms are obtained and THD values are tabulated. From the simulation it is seen that the current harmonics increase with faults in rectifier and inverter module. The THD value increases with faults. For inverter module, the current value increases for Phase A IGBT grounded fault. For rectifier module, the current magnitude remains same. Frequency spectrums under three different fault conditions are distinctly different.

In this work, VSI fed induction motor drive system is simulated. There is a scope for simulating the induction motor drive fed from ZSI and 3 Phase AC Chopper circuits.

## References

- [1] M.E.H. Benbouzid (2000), 'A Review of Induction Motors Signature Analysis as a Medium for Faults Detection,' *IEEE Trans. Industrial Electronics*, vol. 47, no. 5, pp. 984 – 993.
- [2] B.,Biswa, S. Das (2009), 'Current Harmonics Analysis of Inverter-Fed Induction Motor Drive System under Fault Conditions,' in *Proc. of the International MultiConference of Engineers and Computer*.
- [3] Bin Huo and Andrzej M. Trzynadlowski(2001), 'Simple Stator Fault Detector for AC Motors, *IEEE Trans. Industry Applications*,, vol.39, pp. 192-194.
- [4] Debmalya Banerjee, V. T.Ranganathan (2009), ' Load-Commutated SCR Current-Source-Inverter-Fed Induction Motor Drive With Sinusoidal Motor Voltage and Current' *IEEE Transactions on Power Electronics*, vol. 24, no. 4.
- [5] Don.-H. Hwang, K.-C.Lee, Y. -J. Kim (2003), "Voltage stresses on stator windings of induction motors driven by IGBT PWM inverters', in *Proc. 38th IAS Annual conference*, vol. 1, pp. 439 – 444.
- [6] Jee-H Jung, Lee J, and Kwon B (2006), "Online Diagnosis of Induction Motors Using MCSA", *IEEE Trans. Industrial Electronics*, vol. 53, no. 6, pp. 1842 – 1852.
- [7] L. A. Pereira, Silva Gaz G. da zana, and L.F. Pereira (2005), "Motor current signature analysis and fuzzy logic applied to the diagnosis of short-circuit faults in induction motors", in *Proc. 32nd Annual Conference of IEEE Industrial Electronics Society IECON 2005*, pp. 6.
- [8] Shi K.L.,Chan T.F. and Wong Y.K.(1999), ' Modelling And Simulation Of The Three-Phase Induction Motor Using Simulink', in *Proc. Int. J. Elect. Enging. Educ.*, Vol. 36, pp. 163–172. Manchester U.P.
- [9] R.SaravanaKumar K.Vinoth Kumar Dr. K.K.Ray(2009), " Fuzzy Logic based fault detection in induction machines using Lab view", *IJCSNS International Journal of Computer Science and Network Security*, VOL.9 No.9, September 2009.
- [10] Jee-Hoon Jung, Jong-Jae Lee, and Bong-Hwan Kwon(2006), "Online diagnosis of Induction motors using MCSA," *IEEE Trans. Ind. Elec.* 53, no.6, pp.1842-1852, December 2006.